

Concepts for Micro-Pneumatic and Micro-Hydraulic Logic Gates

Albert K. Henning*

Aquarian Microsystems, 199 Heather Lane, Palo Alto, CA USA 94303

ABSTRACT

Previously, we proposed novel microvalve structures, amenable to bulk micromachining, which effected fully complementary behavior in the switching of pneumatic (compressible gas) signals from a high pressure state to a low state, and vice versa. Using our quantitative relations for the flow of compressible gases in microvalves, we described mathematically the steady-state behavior of these micro-pneumatic logic gates, and derived the transfer characteristic for switching between pneumatic states. In this work, we extend the steady-state description to encompass a mathematical treatment of the transient response of micro-pneumatic logic gates. By analogy to MOSFET scaling in integrated circuits, we also apply the full transient model to scaled versions of a micro-pneumatic ring oscillator, in order to illustrate the performance which these devices may afford. As with MOSFETs (which rely on the compressibility of the electron gas), the ultimate speed of these devices is limited by the velocity of sound of the compressible gas. Finally, we present structures which can be used to realize micro-hydraulic logic. In micro-hydraulic logic, because the working fluid is now incompressible, the physical structure must have an alternate means to achieve capacitance, or storage of mass. Such a means is embodied in a variable-volume component attached to each node in the logic circuit.

Keywords: MEMS, microvalve, microfluidics, mass flow control, compact gas flow model, micropneumatic logic, microhydraulic logic

LIST OF VARIABLES

\dot{m}	Mass flow (usually in sccm, normalized to 273 K and 1 atm)
P_c	Control pressure
P_i	Inlet pressure
P_o	Outlet pressure
P_t	Threshold pressure
γ	Ratio of specific heats, c_p/c_v
α	$= \sqrt{\gamma \left(\frac{2}{1+\gamma} \right)^{\frac{\gamma+1}{\gamma-1}}}$
δ	$= \sqrt{\frac{4\gamma}{(\gamma+1)(\gamma-1)}}$
R	Gas constant in $p = \rho RT$ (8314 m ² /K-sec ² divided by molecular weight)
E	Young's modulus for the membrane material
A_s, B_s	Deflection coefficients for the membrane, related to membrane stroke
D	Microvalve inlet diameter
h	Microvalve membrane thickness
a	Microvalve membrane length (of one side)
W	Microvalve seat perimeter length (usually 4*D)
z	Microvalve membrane-to-inlet gap
z_0	Microvalve membrane-to-inlet gap at zero stroke
s	Microvalve membrane stroke

A_{eff}	Microvalve effective flow area
C_d	Microvalve inlet coefficient of discharge
C_v	Microvalve coefficient of flow
ρ	Density of incompressible liquid

1. INTRODUCTION

An analogy between electronic MOSFETs and pneumatic microvalves has recently been suggested [1]. The suggested analogy leads naturally to the notion of a logic element, based on the flow of a compressible (electrically neutral) gas [2]. Neither the notion of a pneumatic logic element [3, 4], nor the flow vs. pressure behavior of a pneumatic microvalve [5], is new. Nonetheless, the extension of the MOSFET-microvalve analogy, to encompass a micro-pneumatic or micro-hydraulic logic element in microvalve form, and the exciting prospects for such elements (for instance, to facilitate microflow or microfluidic arrays, or to enable non-electronic computation in environments hazardous to electronics), warrant substantial further investigation.

Previously, we proposed novel microvalve structures, amenable to bulk micromachining, which effected fully complementary behavior in the switching of pneumatic signals from a PHI pressure state to a PLO state, and vice versa [6]. Using our quantitative relations for the flow of compressible gases in microvalves [7], we described mathematically the static behavior of these micro-pneumatic logic gates, and derived the transfer characteristic for switching between pneumatic states.

In this work, we extend the steady-state description to encompass a mathematical treatment of the transient response of micro-pneumatic logic gates. Following the suggestion of [8], we also apply the full transient model to scaled versions of a micro-pneumatic ring oscillator, in order to illustrate the performance which these devices may afford. Note that, as with MOSFETs, the ultimate speed of these devices is limited by the velocity of sound of the compressible gas.

Finally, we extend the concepts related to micro-pneumatic logic, based on flow of a compressible gas, to cover micro-hydraulic logic, based on the flow of an incompressible liquid. It is shown mathematically that transient behavior of micro-hydraulic logic elements can be achieved by replacing the compressibility of a gas (which leads to capacitance, a necessary element of logic circuits), with the expansion capability of a storage element whose volume varies with pressure. This statement can be given more precisely. In micro-pneumatic logic, mass storage is achieved because the mass in a fixed volume increases as the pressure of the variable density compressible gas inside the volume increases. In micro-hydraulic logic, on the other hand, mass storage is achieved because the mass in a variable volume increases as the pressure of the fixed density incompressible liquid inside the volume increases. Variable volume elements in microfluidic devices are easily realized using flexible membranes.

2. CONCEPTS

A variety of approaches have been made toward the realization of microscale fluidic logic. For the most part, these efforts are not *primary* logic circuits, but *secondary*. That is: in a primary logic device (such as, for instance, a CMOS FET NOR gate), a voltage input results in a voltage output. In virtually every attempt at microfluidic logic, except for Refs. [1, 2, 9, 10], the circuits are *secondary*, insofar as the output is energetically different from the input. For instance, the well-known work in Refs. [11 and 12] accepts a pneumatic input, and delivers an optical output. For the most part, microfluidic logic devices take an electric input, and convert it to a fluidic (usually hydraulic) output, although other modalities (e.g. electrochemical to fluidic) exist [13-17].

It is also important to draw a distinction between *pneumatic* and *hydraulic* behavior in microfluidic logic elements. For the most part, ‘microfluidics’ entails the control and distribution of liquids. ‘Pneumatics’, however, refers to compressible gases, while ‘hydraulics’ refers to incompressible liquids. The distinction is important, and will become clear later in this work, when relatively identical logic structures are used to realize, first, micro-pneumatic logic, and second, micro-hydraulic logic.

Figure 1 portrays a normally-open microvalve. The microvalve has a flexible membrane, whose position z relative to the valve seat is controlled by the difference between control pressure P_c , and the inlet and outlet pressures P_i and P_o . The work in Ref. [7] described the full behavior of microvalve flow, under sonic and subsonic conditions, while accounting for the additional non-linearities of flow as the valve first opens. The membrane deflection s from the equilibrium position z_0 is essential to the control of flow. The membrane thickness is h , the area is a , and the Young's modulus is E . γ is the specific heat ratio for the compressible gas. If an 'edgeless' microvalve is used, then most of the complications associated with inhomogeneous membrane pressure loading (in Ref. [1]) disappear.

It is worth noting that pressure-based mass flow controllers, built using a microvalve and a critical orifice [18], are simply an 'enhancement-depletion' inverter, operated analogically and not digitally.

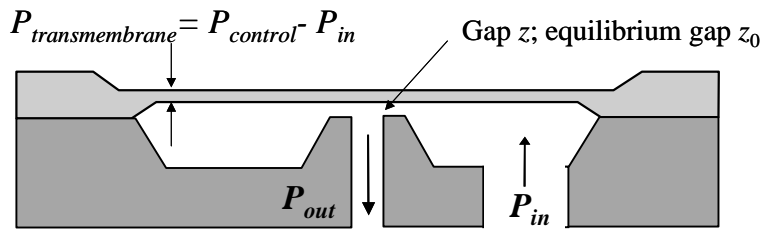


Figure 1: Schematic of a typical normally-open microvalve.

2.1. Normally-closed valve

Figure 2 shows the first basic micro-pneumatic logic element [6]. The microvalve is normally-closed. The central boss, and the construction process, provide an initial tension, which must be overcome by a threshold control pressure before the valve opens. Note that the valve opens only when the difference between the inlet pressure and the control pressure exceeds a threshold value. The quantitative details of the relationship between the threshold pressure and the structural parameters of the valve are found in Ref. [6].

'Edgeless' structures distinguish themselves from the enhancement-depletion devices in Refs. [1, 2]. They enable virtually leak-free behavior when their individual elements are OFF, by placing a smooth membrane against a smooth valve seat. Alternatively, an elastomeric material can be embodied in the valve seat or the membrane boss, in order to retain minimum or zero leakage in the OFF state.

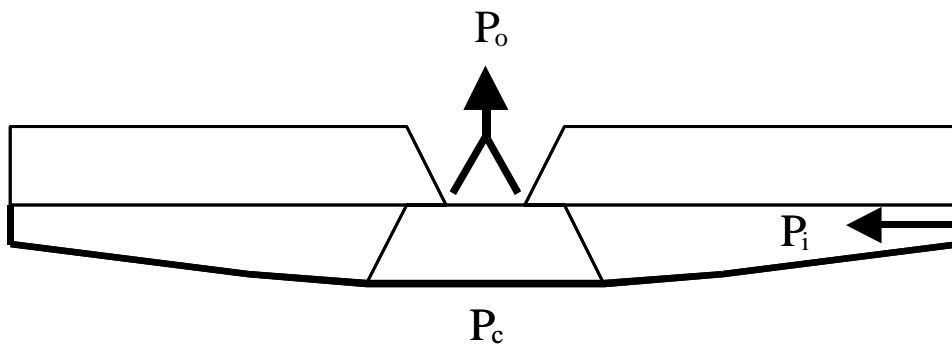


Figure 2: Cross-section of a normally-closed microvalve.

2.2. Normally-closed poppet valve

Figure 3 shows the second basic micro-pneumatic logic element [6]. This microvalve is also normally-closed. However, the central boss is replaced by a poppet structure. The construction process and the poppet structure provide an initial tension, which must be overcome by a threshold control pressure before the valve opens. The quantitative

details of the relationship between the threshold pressure and the structural parameters of the valve are found in Ref. [6]. Note that the valve in this instance opens when the difference between the control pressure and the outlet pressure exceeds a positive threshold value. This relationship seems only subtly different from that of the valve in Fig. 1. However, the difference is crucial to the realization of digital pneumatic or hydraulic logic.

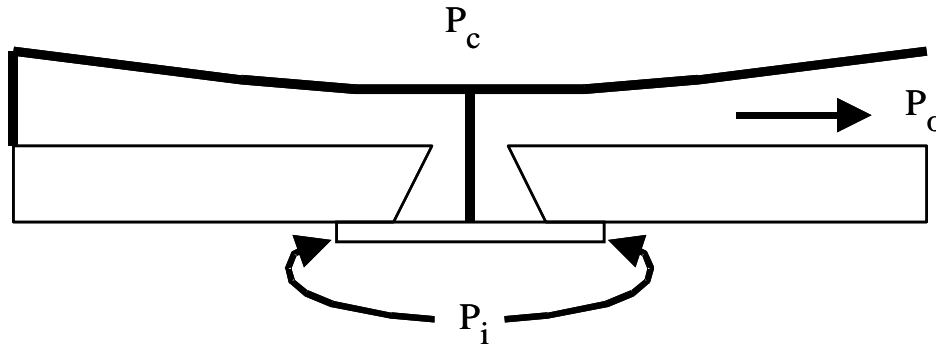


Figure 3: Cross-section of a normally-closed poppet microvalve. Flow directions are indicated by the arrows.

2.3. NOR gate (compressible fluid)

Figure 4 shows two pneumatic logic devices, cascaded together. The cascade allows immediate depiction of the two logic states of this device. Note in particular how the individual valves of Figs. 2 and 3 are connected. That is: in each inverter, the control pressures of the two valves are joined to create a signal input pressure, called PIN; and, the outlet pressure of the valve in Fig. 2 is joined to the inlet pressure of the valve in Fig. 3, to create a signal output pressure called POUT. Using this construction, the logic behavior of the device is readily apparent. Using a source pressure of PHI, and a sink pressure of PLO, and noting in the figure that high pressures are cross-hatched, the first inverter indicates that, for a high signal input pressure, the upper valve remains closed, because the threshold pressure between PHI and PIN has not been exceeded. On the other hand, the lower valve is opened, because the threshold pressure between PIN and PLO has been exceeded. For the right-hand inverter or NOR gate, the situation is reversed. PIN is now low, having been set by the signal output of the left-hand inverter. As a consequence, the upper valve is opened, because the difference between PHI and PIN exceeds the threshold pressure. Meanwhile, the lower valve is closed, because the difference between PIN and PLO is less than the threshold pressure. Figure 5 shows a 3D rendering of a single NOR gate. This view shows plainly how the source and sink pressures PHI and PLO can be brought to bear on the structure. Other logic gates, such as NAND, AND, OR, or XOR, are readily made from the valves of Figs. 2 and 3.

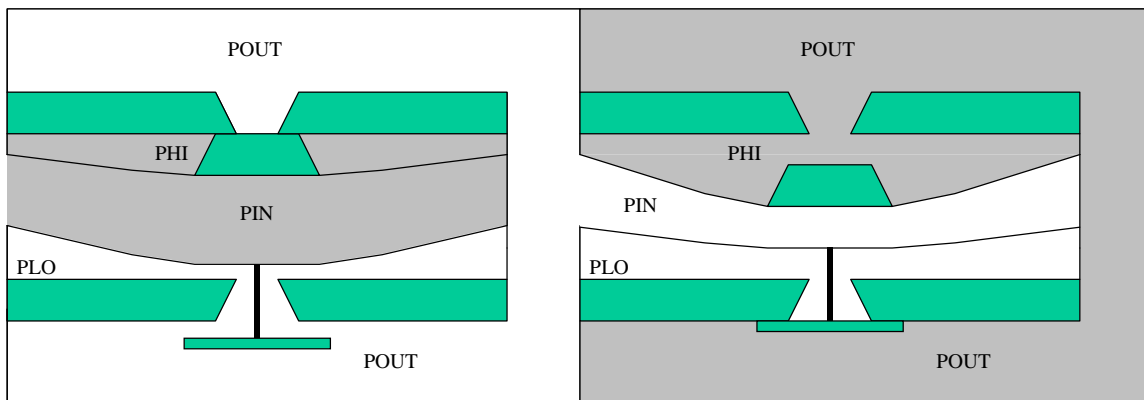


Figure 4: Two cascaded micro-pneumatic logic elements (two inverters). The upper structure in each inverter is a bossed, normally-closed valve, while the lower structure is a normally-closed poppet valve. For each element, the logic signal (a pressure field) arrives from the left, and exits on the right. The ports supplying the PHI and PLO references are out of the plane of this cross-section. The shaded areas are at pressure PHI.

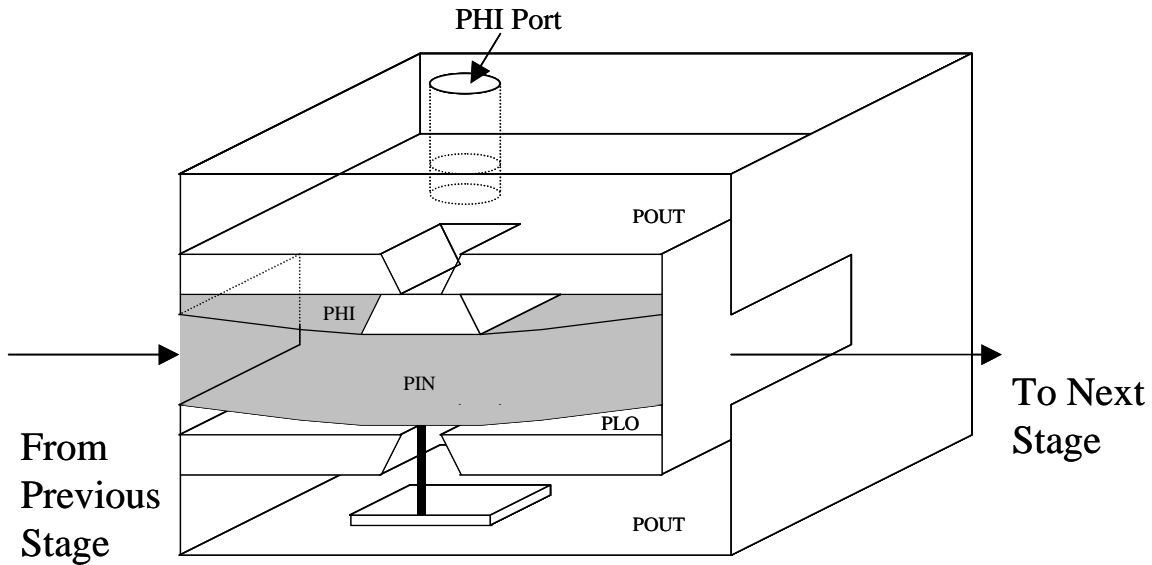


Figure 5: Single micro-pneumatic logic element (inverter) The port supplying the PHI and PLO reference is shown.

2.4. Ring oscillator (compressible fluid)

Figure 6 shows a schematic of the three-element ring oscillator studied previously for its transient response, and presented again here for the sake of completeness. Any similar construction of an odd number of NOR gates, connected in a loop, will result in a oscillation, because the high-low or low-high relationship between the signal input pressure and signal output pressure of any particular stage will always be in flux. The details of modeling of the transient pressure response of this device will be presented in a subsequent section. The structure is completely analogous to the ring oscillators commonly studied in CMOSFET microelectronic circuits, used to characterize a particular fabrication technology, but also useful for purposes of generating oscillating signals in integrated circuits.

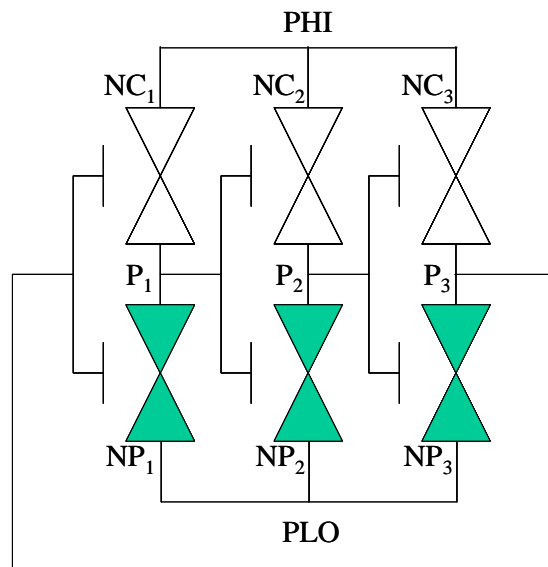


Figure 6: Schematic of three micro-pneumatic logic gates, cascaded in order to create a ring oscillator. Note that the input pressure for Gate 1 is P3; for Gate 2, P1; and for Gate 3, P2. 'NC' is the bossed valve of Figure 2; 'NP' is the poppet valve.

2.5. NOR gate (incompressible fluid)

To realize microhydraulic logic, only a subtle change is required to the basic NOR gate. The component valves from Figs. 2 and 3 remain sufficient to the tasks of acting as the pull-up and pull-down elements of the gate. However, because in microhydraulics the motive fluid is incompressible, the capacitive effect of the compressible gas (the motive fluid in micropneumatic logic) must be replaced by some other mechanism. That is: a compressible gas facilitates storage of mass in the *fixed volume* associated with a pressure node between logic elements. Since storage of mass is required in order to effect logic, if the motive fluid no longer embodies that feature, then another mechanism must be found.

To realize mass storage when using an incompressible fluid, it is simple to alter the microstructure, to incorporate a *variable volume*, and associate such a variable volume with each pressure node in the microhydraulic circuit. Figure 7 depicts how this relatively simple change may be made, by associating a flexible membrane with each pressure node in the logic circuit. The mathematical implication of this replacement will be discussed in the section on modeling.

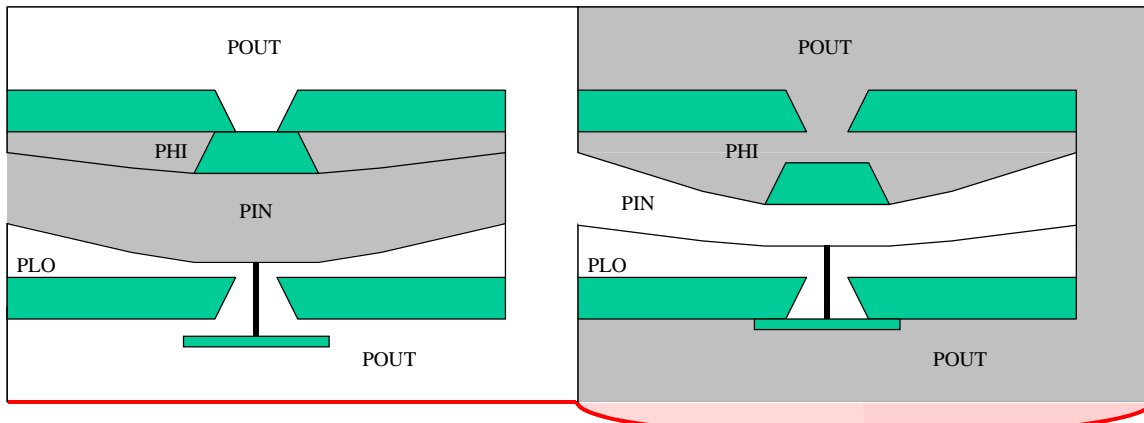


Figure 7: Two cascaded microhydraulic NOR gates (inverters). The upper structure in each inverter is a normally-closed valve, while the lower structure is a normally-closed poppet valve. Access to POUT and PIN is out of the plane of the cross-section shown. The variable volume, or fluidic capacitor, distends when the nodal pressure rises above PLO.

2.6. Ring oscillator (incompressible fluid)

Figure 8 shows the circuit representation of a three-stage microhydraulic ring oscillator. The physical mass storage structures are called out as capacitors. A capacitor is a variable volume, whose volume depends on the nodal pressure.

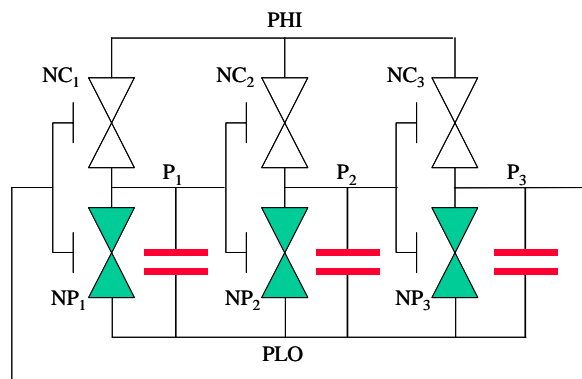


Figure 8: Schematic of three microhydraulic logic gates, cascaded in order to create a ring oscillator. Note that the input pressure for Gate 1 is P3; for Gate 2, P1; and for Gate 3, P2. 'NC' is the bossed valve of Figure 2; 'NP' is the poppet valve. The 'capacitors' are variable volumes; each volume depends on the nodal pressure.

3. MODELING

3.1 Micro-pneumatic models (compressible gases)

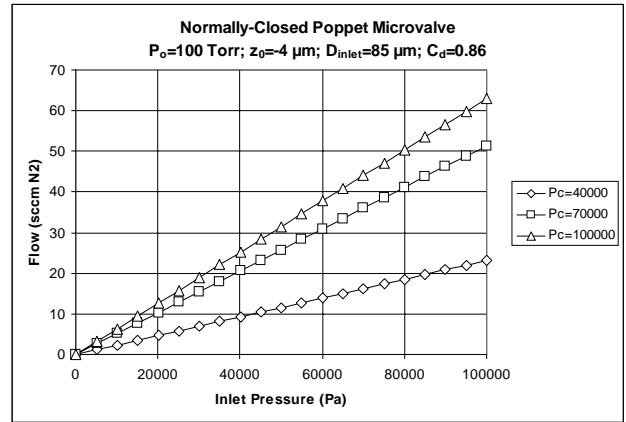
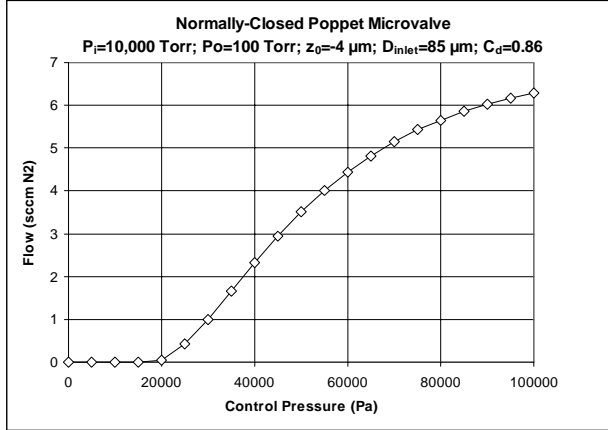
Equations 1 relate the pneumatic boundary conditions, mechanical behavior of a microvalve membrane, and the microvalve flow model for the normally-closed poppet microvalve [6]. Though not elaborated in this work, the sonic and subsonic flow equations have close analogies to, respectively, the saturation and linear equations for electron flow in MOSFETs. Figures 9 and 10 show the results of applying this model to the structure of Fig. 3, using the model (structural, material, and boundary condition) parameters shown in the figure.

$$z = z_0 - s \quad P_t \equiv EA_s \frac{z_0 h^3}{a^4} \frac{(P_c - P_o) a^4}{Eh^4} = A_s \frac{s}{h} + B_s \frac{s^3}{h^3} \Rightarrow \frac{P_{co} a^4}{Eh^4} \cong A_s \frac{s}{h}$$

$$A_{eff} = Wz = W(z_0 - s) = Wa \frac{a^3}{h^3} \frac{1}{A_s E} (P_t - P_{co})$$

$$\dot{m}_{sonic} = C_d C_v \frac{\alpha(\gamma)}{\sqrt{RT}} Wa \frac{a^3}{h^3} \frac{1}{A_s E} (P_t - P_{co}) P_i \quad (1)$$

$$\dot{m}_{subsonic} = C_d C_v \frac{\delta(\gamma)}{\sqrt{RT}} Wa \frac{a^3}{h^3} \frac{1}{A_s E} (P_t - P_{co}) P_i \left(\frac{P_o}{P_i} \right)^{\frac{\gamma+1}{2\gamma}} \sqrt{\left(\frac{P_i}{P_o} \right)^{\frac{\gamma-1}{\gamma}} - 1}$$



Left: Figure 9: Control pressure characteristic for a normally-closed poppet microvalve. The gas is nitrogen, and the gas stagnant temperature is 298 K. Right: Figure 10: Inlet pressure characteristic for the normally-closed poppet microvalve of Figure 6.

If the compressible gas flow model is applied to two valves, one from Fig. 2 and one from Fig. 3, which are combined into the NOR gate structure of Fig. 4, then Figure 11 depicts the resulting transfer characteristic. For this design, the following parameters are employed: silicon is the structural material; the membrane thickness is 50 μm ; the membrane is square, with a side length of 4500 μm ; the temperature is 298 K; the inlet diameter of the upper (normally-closed) valve is 51 μm ; the inlet diameter of the lower (normally-closed poppet) valve is 85 μm ; P_{HI} in the system is 100000 Pa; P_{LO} in the system is 100 Pa; the threshold gaps for each device are -4 μm (the minus sign indicates the tension in the membranes which creates the normally-closed condition). Nitrogen is the working fluid.

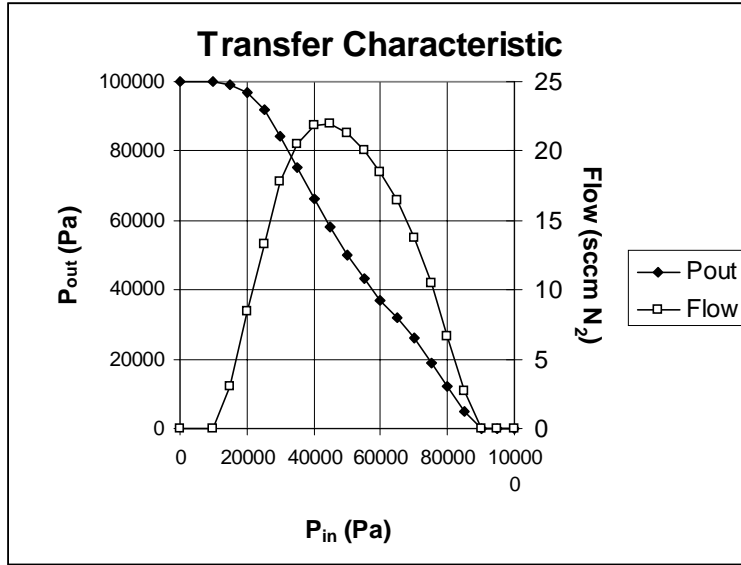


Figure 11: Transfer characteristic for a micro-pneumatic, fully-complementary inverter (NOR gate).

Equations 2 show the mathematical model which accounts for transient effects in Figure 6, due to changes in the nodal pressures associated with the fixed volume between logic elements. These equations arise from applying a control volume around each logic node, such that the additional mass stored at each node (in the form of a compressed gas) arises from the difference between the mass entering the control volume from the normally-closed valve, and exiting the control volume through the normally-closed poppet valve.

$$\begin{aligned} \frac{dP_1}{dt} &= \frac{RT}{V_1} (\dot{m}_{NC1} - \dot{m}_{NP1}) & \frac{dP_2}{dt} &= \frac{RT}{V_2} (\dot{m}_{NC2} - \dot{m}_{NP2}) \\ \frac{dP_3}{dt} &= \frac{RT}{V_3} (\dot{m}_{NC3} - \dot{m}_{NP3}) \end{aligned} \quad (2)$$

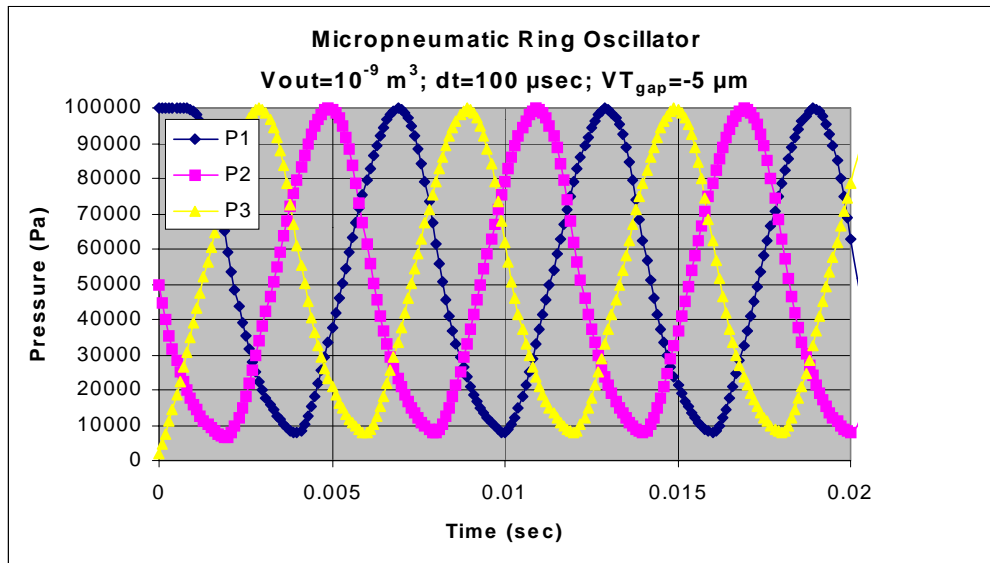


Figure 12: Transient response for a ring oscillator with three logic elements/gates, with the same structural parameters and boundary conditions as in Figure 3. The volume associated with the node between gates is V_{out} , as indicated in the figure. The characteristic transition time is approximately 6 ms. 1.16×10^{-9} kg of nitrogen gas is consumed, per cycle per stage.

Figure 12 shows the transient response of a three-element ring oscillator, using virtually the same model parameters as in the transfer characteristic of Figure 11.

In the spirit of Ref. [8], Figure 13 shows the transient response for a three-element ring oscillator, using scaled values of the model parameters

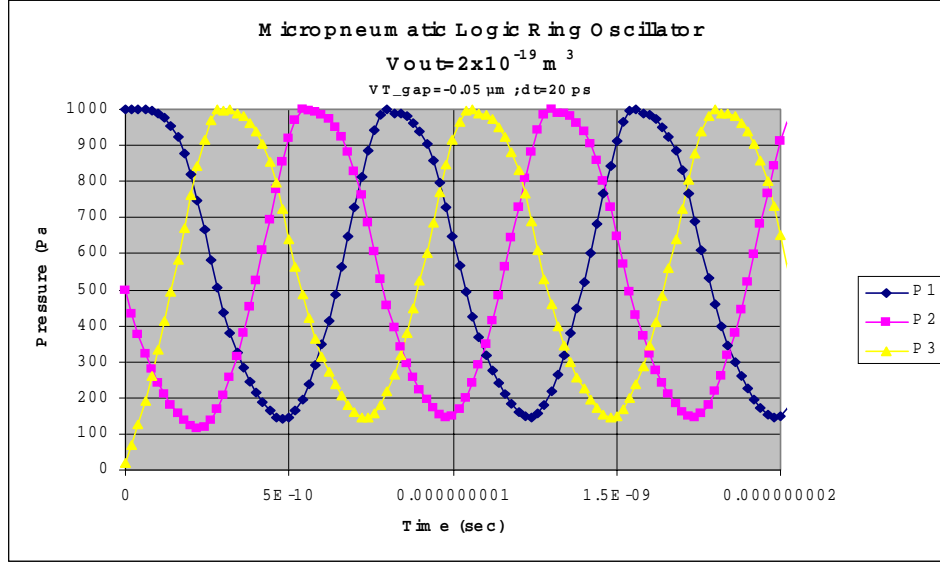


Figure 13: Transient response for a scaled three-stage ring oscillator with the following parameters: membrane thickness $0.2 \mu\text{m}$; side length $90 \mu\text{m}$; $T=298 \text{ K}$; inlet diameter of the upper NC valve is $5.1 \mu\text{m}$; inlet diameter of the lower NP valve is $8.5 \mu\text{m}$; P_{HI} is 1000 Pa ; P_{LO} is 10 Pa ; threshold gaps for each device are -50 nm . The characteristic transition time is approximately 0.75 ns .

3.2 Micro-hydraulic models (incompressible liquids)

Equations 3 show the mathematical model which accounts for transient effects in Figure 8, due to changes in the nodal pressures associated with the variable volume between logic elements. These equations arise from applying a control volume around each logic node, such that the additional mass stored at each node (in the form of an incompressible liquid) arises from the difference between the mass entering the control volume from the normally-closed valve, and exiting the control volume through the normally-closed poppet valve. The liquid flow equation is also called out, where the effective area has the same functional dependence as in Eqs. (1). Also shown is the relationship between the variation of the storage volume, and the stroke of the membrane associated with the storage volume. This membrane is not to be confused with the control membranes in either of the microvalves associated with each logic gate.

$$\begin{aligned}
 \rho \frac{dV_1(P_1)}{dt} &= \dot{m}_{NC1} - \dot{m}_{NP1} & \rho \frac{dV_2(P_2)}{dt} &= \dot{m}_{NC2} - \dot{m}_{NP2} \\
 \rho \frac{dV_3(P_3)}{dt} &= \dot{m}_{NC3} - \dot{m}_{NP3} \\
 \dot{m} &= C_d A_{eff} \sqrt{2\rho\Delta P} \\
 \delta V &\cong 0.38a^2 s \Rightarrow s = \frac{\delta V}{0.38a^2}
 \end{aligned} \tag{3}$$

Figure 14 shows the results of the application of this model to a three-element ring oscillator comprised of micro-hydraulic NOR gates. The structural, material, and boundary condition parameters are identical to those for the micro-pneumatic version of this ring oscillator. The membrane area and thickness for the membrane associated with the mass storage at each node is shown in the figure title. (The initial portion of the curves in Figure 14 is due to the start-up of the model from non-ideal initial conditions of nodal pressure.)

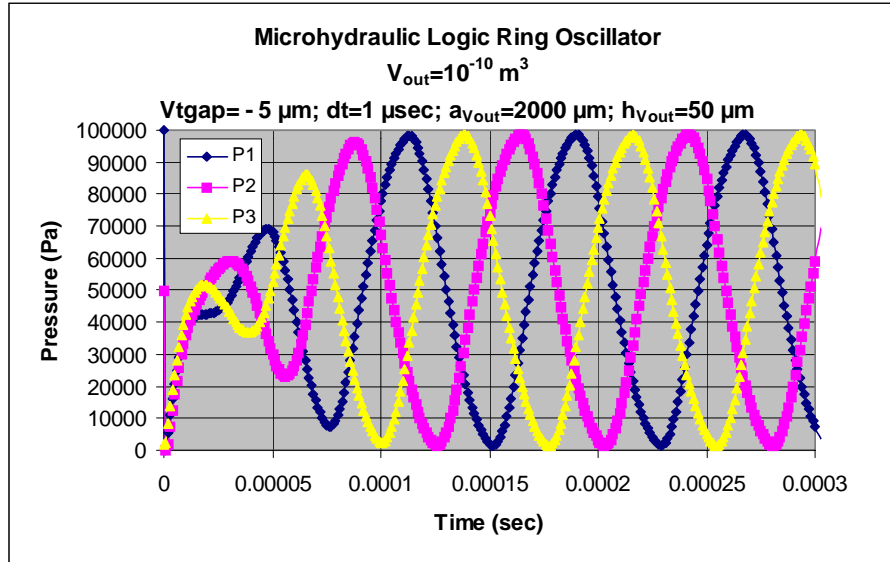


Figure 14: Transient response for a ring oscillator with three logic elements/gates, with the same structural parameters and boundary conditions as in Figure 3. The volume associated with the node between gates is V_{out} , as indicated in the figure. The characteristic transition time is approximately $75 \mu s$. $1.47 \times 10^{-6} \text{ cm}^3$ of liquid water is consumed, per cycle per stage.

4. DISCUSSION

While to a certain extent the results speak for themselves, it is worthwhile to draw attention to a few important features.

The response times for micro-pneumatic and micro-hydraulic ring oscillators, built from identical valve structures, are substantially different. While the size of the fixed volume in the micro-pneumatic model, and the structural variables in the variable volume in the micro-hydraulic model, have a great deal to say about the response time, nonetheless to zeroth order the difference can be attributed to the velocity of sound of the working fluid. So, whether a logic circuit is created from microelectronic MOSFETs, or from the structures described here, the sound velocity of the working fluid (water, gas, or electron gas) always determines the 'speed limit' for performing calculations. This limit arises because the sound velocity is, in a fundamental manner, the speed at which information can be conveyed in the circuit.

So, one would expect that micro-hydraulic circuits would exhibit much improved performance, compared to micro-pneumatic circuits, if both were built according to similar designs. While this expectation will be reasonable at relatively large dimensions, as the fluidic circuits scale, boundary effects will become increasingly important, and will limit performance. That is: microelectronic circuits are based on electron flow through solid materials, and flow is limited primarily by bulk scattering effects, and not boundary scattering. Conversely, microfluidic circuits are largely limited by boundary scattering (due to the boundary layer developed by flow of a fluid through a physical structure). There is, therefore, a surface-area-to-volume ratio effect, and microfluidic devices will suffer more from this effect than will microelectronic devices.

Nonetheless, provided boundary effects are not too limiting, the model predictions for response times in the relatively large micro-hydraulic ring oscillators of Fig. 14 are $75 \mu s$, which is an impressive number. Similarly, for a scaled micro-pneumatic ring oscillator, response times on the order of tens of nanoseconds appear feasible, even for microfabricated structural dimensions quite large compared to present-day integrated circuit microfabrication practice.

Unlike all other reported microfluidic logic structures, the devices reported in Ref. [6] and here are truly complementary. Provided OFF-state leak rates are low, mass (and therefore energy) are only consumed when logic gates are in transition; that is, when the logical state associated with a pressure node is changing value. The amount of mass consumed, even at the relatively large scales of the micro-pneumatic and micro-hydraulic devices modeled here, is extremely small, suggesting that closed-cycle systems could be developed, wherein mass is conserved at the system level, and overall energy is consumed only to pump the supply pressures (PHI and PLO) to relatively constant values. Alternatively, for field situations (harsh environments, or high EM radiation environments) where computation is desirable, but electronic energy cannot be used or is not preferred, micro-pneumatic and micro-hydraulic circuits could easily be operated using hand pumps to maintain pressure; or, through the use of disposable or refillable cartridges of high pressure gas; or, through the evaporation of compact liquid into a high-pressure vapor.

5. CONCLUSIONS

This work builds on our previous efforts related to micro-pneumatic logic. The effect of scaling structural dimensions of micro-pneumatic ring oscillators is modeled and presented. The micro-pneumatic logic concepts are then extended to the realm of micro-hydraulics, to cover the control of incompressible liquids. This extension is facilitated by replacing the mass storage capability of a compressible gas in a fixed volume, with the mass storage capability of an incompressible liquid in a variable volume.

The results represent a substantial step forward toward the goal of microscale logic structures for the control and distribution of both compressible gases and incompressible liquids. Applications in automotive, HVAC, and aerospace engineering, and pharmaceutical or biofluid development, are anticipated.

REFERENCES

1. H. Takao, M. Ishida, and K. Sawada, "A pneumatically actuated full in-channel microvalve with MOSFET-like function in fluid channel network." *J. Microelectromech.* **11**(5), pp. 421-426 (2002).
2. H. Takao and M. Ishida, "Microfluidic integrated circuits for signal processing using analogous relationship between pneumatic microvalves." *J. Microelectromech.* **12**(4), pp. 497-505 (2003).
3. _____, "Pneumatic logic devices pushed." *Electronic Design*, p. 4 (Penton Media, Cleveland, OH, May 24, 1961).
4. D. F. Jensen, H. R. Mueller, and R. R. Schaffer, "Pneumatic diaphragm logic." In *Advances in Fluidics*, pp. 313-338 (Ed. by F. T. Brown, ASME, New York, 1967).
5. C. Vieider, O. Ohman, and H. Elderstig, "A pneumatically actuated micro valve with a silicone rubber membrane for integration with fluid-handling systems." In *Tech. Dig. 8th IEEE Int'l. Conf. Sol. St. Sens. Act.*, pp. 284-286 (IEEE, Piscataway, NJ, 1995).
6. A. K. Henning, "Micro-pneumatic logic." In *Proceedings, ASME IMECE 2004*, Paper IMECE2004-61334 (ASME, New York, 2004).
7. A. K. Henning, "Compact pressure- and structure-based gas flow model for microvalves." In *Proceedings, Materials and Device Characterization in Micromachining* (International Society for Optical Engineering, Bellingham, WA, 2000; Y. Vladimirovsky and P. J. Coane, eds.), volume 4175, pp. 74-81. Also, A. K. Henning, "Improved gas flow model for microvalves." In *Proceedings, TRANSDUCERS 2003: 2003 International Solid State Sensors and Actuators Conference*, pp. 1550-1553 (IEEE Press, Piscataway, NJ, 2003).
8. R. H. Dennard, F. H. Gaensslen, V. L. Rideout, E. Bassous, and A. R. Leblanc, "Design of ion-implanted MOSFETs with very small physical dimensions." *IEEE J. Sol.-St. Circuits* **SC-9**, pp. 256-268 (1974).
9. K. Relyea and S. Leng, "Micro-fluidic ring oscillators." WISP Final Project Report, unpublished (Dartmouth College, Hanover, NH, 1995).
10. W. H. Grover, R. H. C. Ivester, E. C. Jensen and R. A. Mathies, "Development and multiplexed control of latching pneumatic valves using microfluidic logical structures." *Lab Chip* **6**, pp. 623-631 (2006). Also, R. A. Mathies, W. H. Grover, B. Paegel, A. Skelley, E. Lagally, C. N. Liu, and R. Blazej, "Fluid control structures in Microfluidic devices." U.S. Patent Application 20040209354 (October 21, 2004).

11. M. A. Unger, H.-P. Chou, T. Thorsen, A. Scherer, and S. R. Quake, "Monolithic microfabricated valves and pumps by multilayer soft lithography." *Science* **288**, pp. 113-116 (2000).
12. T. Thorsen, S. J. Maerkl, and S. R. Quake, "Microfluidic large-scale integration." *Science* **298**, pp. 580-584 (2002).
13. S. K. Cho, S. K. Fan, H. Moon, and C.-J. Kim, "Toward digital microfluidic circuits: creating, transporting, cutting and merging liquid droplets by electrowetting-based actuation." In *Proc. 15th Int'l. Conf. MEMS*, pp. 32-35 (IEEE, Piscataway, NJ, 2002).
14. W. Zhan and R. M. Crooks, "Microelectrochemical logic circuits." *J. Amer. Chem. Soc.* **125**, pp. 9934-9935 (2003).
15. R. B. Fair, V. Srinivasan, H. Ren, P. Paik, V. K. Pamula, and M. G. Pollak, "Electrowetting-based on-chip sample processing for integrated microfluidics." In *Proc. Int'l. Elec. Dev. Mtg.*, pp. 32.5.1-32.5.4 (IEEE, Piscataway, NJ, 2003).
16. T. Vestad, D. W. M. Marr, and T. Munakata, "Flow resistance for microfluidic logic operations." *Appl. Phys. Lett.* **84**(25), pp. 5074-5075 (2004).
17. Z. Hua, Y. Xia, O. Srivannavit, J.-M. Rouillard, X. Zhou, X. Gao, and E. Gulari, "A versatile microreactor platform featuring a chemical-resistant microvalve array for addressable multiplex syntheses and assays." *J. Micromech. Microeng.* **16**, pp. 1433-1443 (2006).
18. A. K. Henning, J. S. Fitch, J. M. Harris, E. B. Dehan, B. A. Cozad, L. Christel, Y. Fathi, D. A. Hopkins, Jr., L. J. Lilly, W. McCulley, W. A. Weber, and M. Zdeblick, "Microfluidic MEMS for semiconductor processing." *IEEE Transactions on Components, Packaging, and Manufacturing Technology* **B21**, pp. 329-337 (1998).
19. M. DiGiovanni, Flat and Corrugated Diaphragm Design Handbook. (Marcel Dekker, New York, 1989).